Fluorescence anisotropy measurements on a polymer melt as a function of applied shear stress

ARTICLE *in* MACROMOLECULES · JUNE 1992

Impact Factor: 5.8 · DOI: 10.1021/ma00039a031

Fluorescence Anisotropy Measurements on a Polymer Melt as a Function of Applied Shear Stress

Anthony J. Bur,* Robert E. Lowry, Steven C. Roth, Charles L. Thomas, and Francis W. Wang

Polymers Division, National Institute of Standards and Technology, Gaithersburg, Maryland 20899

Received December 3, 1991; Revised Manuscript Received March 5, 1992

ABSTRACT: Polybutadiene tagged with anthracene was synthesized and used as a fluorescent molecular probe to study shear-induced orientation in a matrix polymer melt. With the tagged polybutadiene doped into a polybutadiene matrix at 0.1% concentration, steady-state fluorescence anisotropy measurements were carried out under zero shear and under finite shear conditions using an optically instrumented cone and plate rheometer. Measurements were made over a shear rate range for which the specimen displayed non-Newtonian behavior, 2.64×10^{-3} to 5.3 s^{-1}. Anisotropy was observed to decrease with increasing applied shear stress. The magnitude of the effect is small and is attributed to shear-induced orientation of the probe molecule which is engaged in the entanglement network of the host polymer. Diluting the entanglement network using plasticizer produced a smaller effect. For polybutadiene plasticized with 50% cetane, we observed that anisotropy was independent of the applied shear stress, indicating that the probe molecule was not participating in the orientation of the matrix entanglement network. A relationship between anisotropy, chromophore relaxation time, and orientation factors was derived and used to deduce an orientation distribution of fluorescent absorption dipoles and to illustrate the difference between shear and extension stress observations. Extension experiments, carried out using a cross-linked polybutadiene specimen, showed that anisotropy increased as a function of applied extensional stress.

Introduction

Fluorescence anisotropy measurements have been employed by many authors to explore both molecular relaxation times and molecular orientation. Dynamic depolarization measurements of solutions of polymers tagged with fluorophores have been used to examine molecular relaxation models.[1-4] Steady-state anisotropy measurements have yielded orientation functions for highly extended polymers and cross-linked rubber.[5-8]

We consider anisotropy r obtained as depicted in Figure 1 from excitation light beam traveling in the positive y direction with a fluorescence detector situated at zero degrees with respect to this beam. The anisotropy relationship of interest to us is

$$r = \frac{I_{zz} - I_{zx}}{I_{zz} + 2I_{zx}} \tag{1}$$

where I_{zz} is the intensity of the fluorescence when the excitation light is polarized along the z direction and the fluorescence analyzer is also oriented in the z direction, and I_{zx} is the intensity obtained with the analyzer directed along the x axis.

In general, anisotropy will depend on molecular orientation, fluorescence decay time τ_f, and the rotational relaxation time of the probe τ_r. Theoretical models of anisotropy which take into account these quantities have been carried out by several authors.[6,9-12] In all of the published work, uniaxial orientation was assumed, a situation applicable to extensional strain, liquid crystals, and fibers. The symmetry of uniaxial orientation does not apply in the case of shear flow, but published work provides a framework for extending the models. Below, we present a calculation of the time-dependent anisotropy decay $r(t)$ of a photoselected ensemble of fluorophores in an environment having no spatial symmetry.

Experimentally, our primary objective has been to use fluorescence anisotropy measurements to monitor shear-induced polymer molecular orientation. To do this, we synthesized a fluorescent probe molecule consisting of polybutadiene tagged with anthracene. This probe has the potential to participate in the entanglement network of a host polymeric matrix and thereby orient with the matrix under applied shear stress. In the experiments described below, anisotropy of the tagged polybutadiene, doped into a polybutadiene matrix, was measured as a function of applied shear stress over a range of shear rates for which the matrix material displayed non-Newtonian behavior. We also investigated the effect of diluting the entanglement network by adding plasticizer, and we examined the effect of extensional stress by preparing cross-linked specimens and measuring anisotropy as a function of applied extensional stress. A preliminary paper regarding this work has been published.[13]

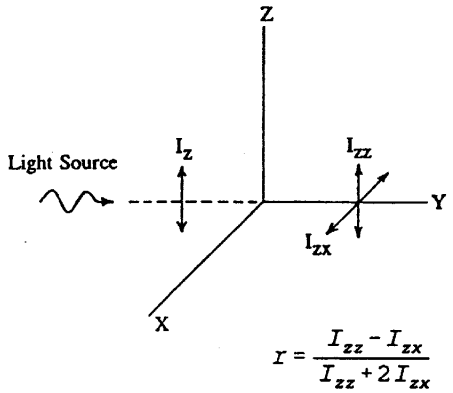

Figure 1. Fluorescence anisotropy defined in relation to the coordinate system established for the experiment.

Theory

We calculate $r(t)$ by considering an ensemble of fluorescent probe molecules undergoing steady-state shear loading. At a constant shear rate, the ensemble assumes an orientation distribution $f(\theta,\phi)$ and θ and ϕ are polar coordinates measured from the z and x axes (see Figure 2). A short pulse of excitation light polarized in the z direction creates a photoselected population of excited

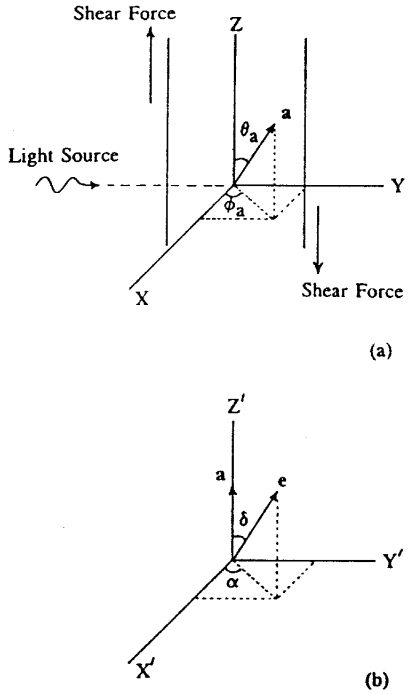

Figure 2. (a) Laboratory coordinate frame of reference. a is the absorption dipole of the fluorophore. (b) Molecular coordinate frame. e is the emission dipole of the fluorophore.

fluorophores with orientation distribution $g(\theta,\phi)$. If the molecular rotational relaxation time τ_r is much greater than the fluorescence decay time τ_f, then $g(\theta,\phi)$ will remain constant during the time window for fluorescence observations. On the other hand, if $\tau_r \approx \tau_f$, then the orientation of the photoselected population will decay with time via the characteristic molecular dynamics of the system; as $t \rightarrow \infty$, $g(\theta,\phi)$ must decay to the steady-state distribution $f(\theta,\phi)$. In the experiment, we do not measure $g(\theta,\phi)$ directly, but we can measure $r(t)$ which depends upon the orientation factors of $f(\theta,\phi)$.

Fluorescence anisotropy decay can be expressed as

$$r(t) = r(\infty) + [r(0) - r(\infty)]\Psi(t) \qquad (2)$$

where $\Psi(t)$ is a relaxation decay function which describes the molecular dynamics associated with the anisotropy decay from its initial value $r(0)$ to $r(\infty)$, the limit of r as $t \rightarrow \infty$. For a randomly oriented distribution of fluorophores, $r(0) = {}^2/_5$ and $r(\infty) = 0$. But, for a permanently oriented system or a system undergoing steady-state orientation stresses, the initial and final values will depend on the orientation factors. Following an approach taken by Szabo,[12] we derive expressions for $r(0)$ and $r(\infty)$ using Wigner rotation matrices and properties of the autocorrelation function. This approach allows us to obtain the two end points of the decay without specifying the dynamics of the molecular motion. Equation 2 is then applied to portray $r(t)$. Since we do not solve the equation of molecular motion, information about the distribution of, or the number of, discrete relaxation times is not obtained. Instead, we rely on published models of molecular relaxation in polymeric materials and on our experimental observations to describe the general features of the molecular relaxation.

Figure 2a shows an absorption dipole moment a of a fluorophore oriented at position (θ_a,ϕ_a). Upon the occurrence of fluoresence, light energy absorbed by a is emitted with a characteristic fluorescence decay time by an emission dipole e (not shown in Figure 2a) oriented at (θ_e,ϕ_e). We also define a molecular coordinate system shown in Figure 2b with a pointing in the z' direction and e oriented at (δ,α). This molecular frame of reference is appropriate for those fluorescent molecules having a directed along a molecular axis of symmetry, e.g., anthracene, the fluorophore which we use in this experimental study.

The probability that light polarized in the z direction will be absorbed by the fluorophore is proportional to $\cos^2\theta_a$. The probability that light emitted by the emission dipole will have polarization in the z direction is proportional to $\cos^2\theta_e$. The observable I_{zz} is obtained from the ensemble average of the product of probabilities that excitation light will be absorbed at time $t = 0$ and that, at a later time t, light emission will occur. Thus

$$I_{zz} \propto \langle \cos^2\theta_a(0)\cdot\cos^2\theta_e(t)\rangle \qquad (3)$$

Similarly, I_{zx} is expressed as the product of absorption and emission probabilities

$$I_{zx} \propto \langle \cos^2\theta_a(0)\cdot\sin^2\theta_e(t)\cos^2\phi_e(t)\rangle \qquad (4)$$

In order to express the r in terms of orientation factors of θ_a and ϕ_a, coordinate transformations from the molecular to laboratory frame of reference must be carried out. We accomplish this using Wigner rotation matrices, a convenient mathematical tool for doing this.[12,14,15] I_{zz} becomes

$$I_{zz} \propto \left\langle \left(\frac{2}{3}D^2_{00}(\Omega_{LA}(0)) + \frac{1}{3}\right)\left(\frac{2}{3}D^2_{00}(\Omega_{LE}(t)) + \frac{1}{3}\right)\right\rangle \qquad (5)$$

where Ω_{LA} and Ω_{LE} represent Euler angles (α,β,γ) and (α',β',γ') for rotation between the laboratory and absorption coordinate frame and the laboratory and emission coordinate frame and D^2_{00} is the rotation matrix. $D^2_{00}(\Omega_{LE})$ can be expressed as rotations first via Ω_{LA} and then Ω_{AE}

$$D^2_{00}(\Omega_{LE}) = \sum_{m=-2}^{2} D^2_{0m}(\Omega_{LA})\, D^2_{m0}(\Omega_{AE}) \qquad (6)$$

where Ω_{AE} represents the Euler rotation angles $(\alpha'',\beta'',\gamma'')$ between the absorption and emission coordinate systems.

We make a simplifying assumption that cylindrical symmetry exists in the molecular coordinate system (Figure 2b); i.e., fluorescence behavior is independent of angle α. For a molecule possessing planar symmetry, such as anthracene, this assumption is an approximation. Cylindrical symmetry is expressed by setting $m = 0$. Equation 6 becomes

$$D^2_{00}(\Omega_{LE}) = \delta_{m0}D^2_{00}(\Omega_{LA})\, D^2_{00}(\Omega_{AE}) \qquad (7)$$

where

$$D^2_{00}(\Omega_{LA}) = P_2(\cos\theta_a) = (3\cos^2\theta_a - 1)/2 \qquad (8)$$

and

$$D^2_{00}(\Omega_{AE}) = P_2(\cos\delta) = (3\cos^2\delta - 1)/2 \qquad (9)$$

and P_2 is the second Legendre orientation term.

I_{zz} becomes

$$I_{zz} \propto \frac{4}{9}P_2(\cos\delta)\langle D^2_{00}(\Omega_{LA},0)\cdot D^2_{00}(\Omega_{LA},t)\rangle + \frac{2}{9}\langle D^2_{00}(\Omega_{LA})\rangle + \frac{2}{9}P_2(\cos\delta)\langle D^2_{00}(\Omega_{LA})\rangle + \frac{1}{9} \qquad (10)$$

where the first term is an autocorrelation function describing the fluorescence decay due to orientation rotation of the fluorophore.

When expressed in Wigner rotation matrix notation, I_{zx} becomes

$$I_{zx} \propto \left\langle \frac{1}{2}\left[\frac{2}{3}D^2_{00}(\Omega_{LA},0) + \frac{1}{3}\right]\left[\left(\frac{2}{3}\right)^{1/2}D^2_{20}(\Omega_{LE},t) + \left(\frac{2}{3}\right)^{1/2}D^2_{-20}(\Omega_{LE},t) - \frac{2}{3}D^2_{00}(\Omega_{LE},t) + \frac{2}{3}\right]\right\rangle \quad (11)$$

$D^2_{mn}(\Omega_{LE})$ can be expressed in terms of Ω_{LA} by the following relation:

$$D^2_{20}(\Omega_{LE}) = \sum_{m=-2}^{2} D^2_{2m}(\Omega_{LA})\, D^2_{m0}(\Omega_{AE}) \quad (12)$$

But, because we have assumed cylindrical symmetry for the probe molecule, eq 12 becomes

$$D^2_{20}(\Omega_{LE}) = \sum_{m=-2}^{2} D^2_{2m}(\Omega_{LA})\, \delta_{m0} D^2_{m0}(\Omega_{AE}) \quad (13)$$

$$= D^2_{20}(\Omega_{LA})\, P_2(\cos\delta) \quad (14)$$

where we have used $D^2_{00}(\Omega_{AE}) = P_2(\cos\delta)$.

In a similar manner, i.e., assuming cylindrical molecular symmetry, $D^2_{-20}(\Omega_{LE})$ and $D^2_{00}(\Omega_{LE})$ become

$$D^2_{-20}(\Omega_{LE}) = D^2_{-20}(\Omega_{LA})\, P_2(\cos\delta) \quad (15)$$

and

$$D^2_{00}(\Omega_{LE}) = D^2_{00}(\Omega_{LA})\, P_2(\cos\delta) \quad (16)$$

I_{zx} becomes

$$I_{zx} \propto \left\langle \frac{1}{2}\left(\frac{2}{3}\right)^{3/2}P_2(\cos\delta)\left[D^2_{00}(0)\cdot D^2_{20}(t) + D^2_{00}(0)\cdot D^2_{-20}(t) - \left(\frac{2}{3}\right)^{1/2}D^2_{00}(0)\cdot D^2_{00}(t)\right] + \left(\frac{2}{3}\right)^2 D^2_{00} + \frac{1}{3}\left(\frac{2}{3}\right)^{1/2}D^2_{20}P_2(\cos\delta) + \frac{1}{3}\left(\frac{2}{3}\right)^{1/2}D^2_{-20}P_2(\cos\delta) - \frac{2}{9}D^2_{00}P_2(\cos\delta) + \frac{2}{9}\right\rangle \quad (17)$$

where it is understood that the argument of the D_{mn} terms is Ω_{LA}. The first three terms in eq 17 are autocorrelation functions which express the time dependence of I_{zx}.

The fluorescence anisotropy decay is obtained by substituting eq 10 and 17 into eq 1. This yields a decay function in terms of the autocorrelation functions but does not express the specific dynamics of the decay. We will use eqs 1, 10, and 17 to obtain values of the anisotropy at $t = 0$ and in the limit as $t \to \infty$ by applying the properties of the autocorrelation function

$$\langle A(0)\cdot B(t)\rangle = \langle A\cdot B\rangle, \quad \text{at } t = 0 \quad (18)$$

and

$$\lim_{t\to\infty}\langle A(0)\cdot B(t)\rangle = \langle A\rangle\cdot\langle B\rangle \quad (19)$$

Using eqs 18 and 19, we are able to evaluate the anisotropy at the end points of the decay without a detailed knowledge of the molecular dynamics of the fluorophore rotational relaxation. At $t = 0$ and in the limit $t \to \infty$, the autocorrelation functions of eqs 10 and 17 become

$$\langle D^2_{00}(\Omega_{LA},0)\cdot D^2_{00}(\Omega_{LA},0)\rangle = \left\langle\left[\frac{3\cos^2\theta_a - 1}{2}\right]^2\right\rangle = \langle[P_2(\cos\theta_a)]^2\rangle \quad (20)$$

$$\lim_{t\to\infty}\langle D^2_{00}(\Omega_{LA},0)\cdot D^2_{00}(\Omega_{LA},t)\rangle = \langle P_2(\cos\theta_a)\rangle^2 \quad (21)$$

$$\langle[D^2_{00}(\Omega_{LA},0)]\cdot[D^2_{20}(\Omega_{LA},0) + D^2_{-20}(\Omega_{LA},0)]\rangle = \left\langle P_2(\cos\theta_a)\cdot\left(\frac{3}{2}\right)^{1/2}\sin^2\theta_a\cos 2\phi_a\right\rangle \quad (22)$$

$$\lim_{t\to\infty}\langle[D^2_{00}(\Omega_{LA},0)]\cdot[D^2_{20}(\Omega_{LA},t) + D^2_{-20}(\Omega_{LA},t)]\rangle = \langle P_2(\cos\theta_a)\rangle\cdot\left\langle\left(\frac{3}{2}\right)^{1/2}\sin^2\theta_a\cos 2\phi_a\right\rangle \quad (23)$$

where the angle ϕ_a is as defined in the laboratory coordinate frame.

By combining eqs 10, 17, 20, and 22, into eq 1, we calculate an expression for the initial anisotropy $r(0)$

$$r(0) = \frac{[2\langle P_2^2\rangle + \langle P_2\rangle - \langle P_2\sin^2\theta_a\cos 2\phi\rangle - 1/2\langle\sin^2\theta_a\cos 2\phi\rangle]P_2(\cos\delta)}{2\langle P_2\rangle + 2\langle P_2\sin^2\theta_a\cos 2\phi\rangle + \langle\sin^2\theta_a\cos 2\phi\rangle P_2(\cos\delta) + 1} \quad (24)$$

where $P_2 = P_2(\cos\theta_a)$ and $\phi = \phi_a$. For random orientation distribution, eq 24 reduces to the appropriate value, $(2/5)[P_2(\cos\delta)]$, or to $^2/_5$ when $\delta = 0$.

$r(\infty)$ is obtained by combining eqs 10, 17, 21, and 23 into eq 1. Thus

$$r(\infty) = \frac{[2\langle P_2\rangle^2 + \langle P_2\rangle - \langle P_2\rangle\langle\sin^2\theta_a\cos 2\phi\rangle - 1/2\langle\sin^2\theta_a\cos 2\phi\rangle]P_2(\cos\delta)}{2\langle P_2\rangle + 2\langle P_2\rangle\langle\sin^2\theta_a\cos 2\phi\rangle P_2(\cos\delta) + \langle\sin^2\theta_a\cos 2\phi\rangle P_2(\cos\delta) + 1} \quad (25)$$

For random orientation, eq 25 equals zero, the value that $r(\infty)$ must be for a random distribution of fluorophores.

Equations 24 and 25, when substituted into eq 2, yield an anisotropy decay function which can be used to describe time-resolved observations. However, our measurements of anisotropy were carried out using continuous illumination. For these conditions, r_{cw} is obtained by integrating over time

$$r_{cw} = r(\infty) + \int_0^\infty [r(0) - r(\infty)]\Psi(t)\cdot\frac{e^{-t/\tau_f}}{\tau_f}\,dt \quad (26)$$

where τ_f is the fluorescence decay time and the term $e^{-t/\tau_f}/\tau_f$ is the probability for fluorescence decay at time t. We obtain

$$r_{cw} = r(\infty) + [r(0) - r(\infty)]A \quad (27)$$

where A is a constant, the result of integrating eq 26 over time. If we assume the simple case of a monoexponential relaxation decay function

$$\Psi(t) = e^{-t/\tau_r} \quad (28)$$

and eq 27 becomes

$$r_{cw} = r(\infty) + [r(0) - r(\infty)](\tau_f/\tau_r + 1)^{-1} \quad (29)$$

where τ_r is the rotational relaxation time of the fluorescent probe. For random orientation, eq 29 reduces to

$$r_{cw} = (2/5)(\tau_f/\tau_r + 1)^{-1}P_2(\cos\delta) \quad (30)$$

which is Perrin's equation for depolarization due to rotational orientation of a spherical fluorophore in an isotropic medium.[16]

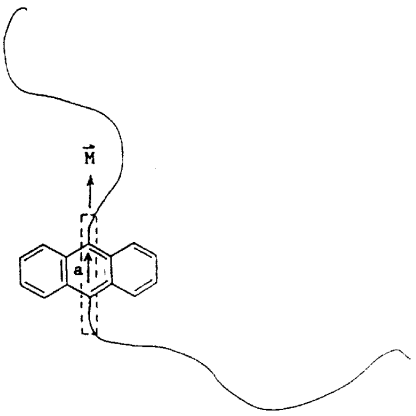

Figure 3. Anthracene-tagged polybutadiene molecule. The strings represent the polybutadiene backbone.

If we assume uniaxial symmetry about the z axis, then $\langle \cos 2\phi \rangle = 0$ and eqs 24 and 25 reduce to those obtained by Szabo[12]

$$r(0) = \frac{[2\langle P_2^2 \rangle + \langle P_2 \rangle]P_2(\cos \delta)}{2\langle P_2 \rangle + 1} \tag{31}$$

$$r(\infty) = \langle P_2 \rangle P_2(\cos \delta) \tag{32}$$

For analysis of our experimental data, we will refer to eqs 24, 25, and 27. We note that these equations were derived making the assumptions that the adsorption dipole a is coincident with the molecular axis z' and that the fluorophore possesses cylindrical symmetry.

Experimental Procedure

Materials. The tagged polybutadiene (PB) probe molecule was derived from bifunctional anthracene which was covalently bonded by ester linkages to polybutadiene chains so that the fluorescent anthracene resides at a central position on the polymer main chain as depicted in Figure 3. The starting materials were dicarboxyl-terminated polybutadiene with a molecular weight of 16 000 and 9,10-anthracenedicarboxaldehyde. The anthracenedicarboxaldehyde was converted to anthracenedimethanol and subsequently covalently bonded to the dicarboxyl-terminated polybutadiene via an esterification reaction. The synthesized product was characterized using gel permeation chromatography (GPC) and infrared analysis. Infrared spectra showed that the conversion of dicarboxyl-terminated anthracene to anthracenedimethanol resulted in the elimination of the carboxyl absorption at 1280 cm^{-1} and the creation of the C–O stretch of the alcohol. Confirmation of the esterification reaction was obtained from the observation of the ester carboxyl line at 1734 cm^{-1}. GPC data showed that the tagged polybutadiene has a molecular weight of 30 000, which is approximately twice that of the starting polybutadiene, and its molecular weight distribution is somewhat broader. We concluded that there is one anthracene per polymer chain and that it is positioned in the center of the main chain as shown in Figure 3.

The matrix polymer material was 420 000 molecular weight polybutadiene, 36% cis, 55% trans, and 9% vinyl, which was obtained from Scientific Polymer Products.[17] Specimens of polybutadiene, containing 5, 17, 50 and 80% plasticizer, were prepared using cetane (hexadecane) as plasticizer. Both plasticizer and the tagged polybutadiene were mixed with the matrix polybutadiene using a common solvent, cyclohexane. The tagged polybutadiene probe was added at 0.1% concentration by weight of polybutadiene and cetane. Thin sheets of these specimens were prepared by pouring the solutions onto a flat surface and slowly evaporating the cyclohexane, leaving behind the less volatile cetane as a plasticizer. One effect of using the plasticizer was increased tackiness of the material which produced improved contact with the cone and plate surfaces.

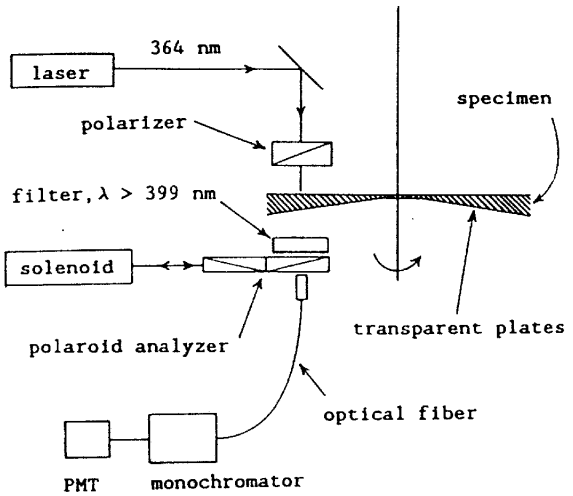

Figure 4. Experimental arrangement for rheometer optics. The excitation wavelength was 364 nm.

A control specimen consisting of 10% cetane-plasticized PB doped with free anthracene was prepared. This specimen was used to compare with the anisotropy measurements on the same matrix polymer doped with the tagged PB probe. Since the low molecular weight anthracene cannot engage in the entanglement network of the matrix polymer, effects due to the absence of entanglements can be observed.

A neat PB specimen doped with the tagged PB probe was cross-linked using γ radiation. An irradiation dose of 21.0 Mrad produced a cross-linked network with an average molecular weight between cross-links $M_c = 1500$ as determined from solvent swelling measurements. The value of M_c is compared with $M_w = 30\,000$ for tagged PB and with $M_e = 2000$–3000, the entanglement molecular weight for PB.[18] This specimen was used to measure anisotropy as a function of the applied extensional stress.

Instrumentation. Simultaneous measurements of rheological parameters and fluorescence anisotropy were obtained by combining a Weissenberg rheogoniometer with anisotropy optics.[17] A diagram of the experimental arrangement is shown in Figure 4. The transparent cone and plate materials of the rheometer were quartz for the upper plate and poly(methyl methacrylate) for the bottom cone; the cone and plate were 7.6 cm in diameter. The Weissenberg rheometer was operated over a wide range of shear rates (10^{-3}–10^{2} s^{-1}) and shear stresses (10^{2}–10^{5} N/m^2).

The essential elements of the optics were the argon ion laser light source, the transparent cone and plate of the rheometer, a unit structural mount for the polarizer and analyzer at the rheometer, the optical fiber cable for fluorescence collection, and the monochromator with a photomultiplier detector. The 364-nm line was selected from the laser for excitation of anthracene. The beam was directed through a crystal polarizer to the specimen with polarization parallel to the tangential velocity of the rotating cone. Perpendicular and parallel components of the fluorescence were obtained using the analyzer which consists of two adjacent pieces of polaroid sheet oriented 90° with respect to each other and aligned with the axis of the polarizer. During the measurement, the two analyzers were sequentially placed in front of the optical fiber collection cable by a computer-driven solenoid. The alignment of the optical components was maintained by a custom-designed optical mount attached to the base of the rheometer. The optical and rheometer coordinate systems were brought into coincidence by referencing the position of the mounting piece to the axis of cone and plate rotation. The 399-nm cut-on filter (see Figure 4) which was placed before the analyzer served two purposes: first, it protected the polaroid analyzer from damaging UV radiation of the excitation light beam; and, second it prevented the excitation beam from entering the optical fiber which is fluorescently active under ultraviolet excitation. Since anthracene fluorescence occurs over a wavelength range from 410 to 510 nm, the filter did not affect the transmission of the desired fluorescence.

Because the cone, plate, and 399-nm cut-on filter were in positions to change the polarization and/or intensity of the desired fluorescence from anthracene, their fluorescence properties and their ability to alter polarization were investigated. We found that the fluorescence from these components was negligible and that the combined effect on polarization was less than 0.5%.

The optical cable consisted of a bundle of 50-μm fibers packed into a cylinder 3 mm in diameter at the collection end and shaped into a slit 1 mm by 5 mm at the exit end where it connected to the monochromator. The optical fiber was found to be an effective polarization scrambler so that a polarization correction of the grating monochromator transmission characteristics was unnecessary. During the anisotropy measurements, the monochromator was set at 428 nm, corresponding to peak fluorescence from anthracene-tagged polybutadiene. The monochromator band-pass was measured to be 12 nm, but since the anisotropy of anthracene is independent of wavelength in the vicinity of 428 nm, the size of the band-pass was not a significant factor. Calibration of the instrument was carried out at zero shear using reference specimens whose anisotropies were measured using a commercial fluorimeter.

Measurement Procedures. The specimens, either concentrated solutions, plasticized sheets, or neat PB, were placed on the bottom cone of the rheometer and compressed to the proper separation between cone and plate. Under this compression, the material flowed beyond the cone/plate edges and eluded bubbles with it. With the solutions, the specimen loading compression relaxed immediately and the proper cone and plate separation was set. For the plasticized and neat materials, whose viscosities were on the order of 10^7 Pa-s, long compression strain relaxation times caused a wait of several days before the cone and plate reached the correct separation.

All measurements were made at room temperature. Two or three decades of shear rate was scanned for each specimen. Upon reaching a steady-state shear stress at each shear rate, anisotropy measurements were made by alternately switching the analyzer from 0 to 90°. Photon-counting times at each position of the analyzer were 0.5 s. Longer counting times were avoided because significant photobleaching of anthracene occurred. At each shear rate setting, at least 30 anisotropy measurements were made yielding an anisotropy value with a standard deviation of 0.0015 or less.

Measurement of $\langle\cos^2\delta\rangle$. A value of $\langle\cos^2\delta\rangle$ was obtained by measuring anisotropy of the tagged polybutadiene under conditions such that anthracene was randomly oriented in space, $\tau_f/\tau_r \ll 1$ and $(\tau_f/\tau_r + 1)^{-1} = 1$ or $A = 1$. For this case, eq 30 becomes

$$r_0 = \frac{2}{5}\frac{3\cos^2\delta - 1}{2} \qquad (33)$$

Experimentally, the situation described by eq 33 was achieved by incorporating the tagged polymer into the glass matrix of poly(methyl methacrylate) at very dilute concentrations, 0.1% by weight. The specimen was prepared by mixing the tagged polybutadiene with methyl methacrylate monomer which was subsequently polymerized. After polymerization, the specimen was cut into the shape of a standard cuvette with a rectangular cross section, 1 cm by 1 cm by 4 cm in length, and its sides were polished. Anisotropy was measured using a commercial fluorimeter. As a check on our sample preparation technique, we also incorporated free anthracene into the PMMA matrix and found that our measurement of r_0, 0.24, agrees with that obtained by Monnerie and co-workers.[2] For tagged polybutadiene in poly(methyl methacrylate), we found $r_0 = 0.22$ or $P_2(\cos\delta) = 0.55$. This value, while close to that for free anthracene, indicates some change in the electronic structure of anthracene in the tagged state compared to that of the free state.

Results

The rheological characteristics of the plasticized specimens are expressed in the viscosity vs shear rate data of Figure 5. Polybutadiene specimens plasticized with 5, 17, and 50% cetane are designated as 95/5, 83/17, and 50/50, respectively. Over the shear rate range investigated, the

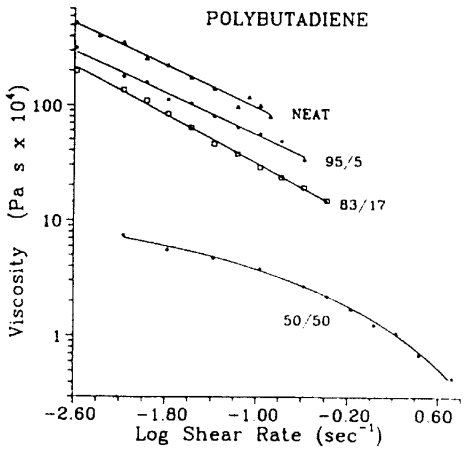

Figure 5. Viscosity versus shear rate plotted for four PB specimens. The designations 95/5, 83/17, and 50/50 refer to PB which was plasticized with 5, 17, and 50% cetane, respectively.

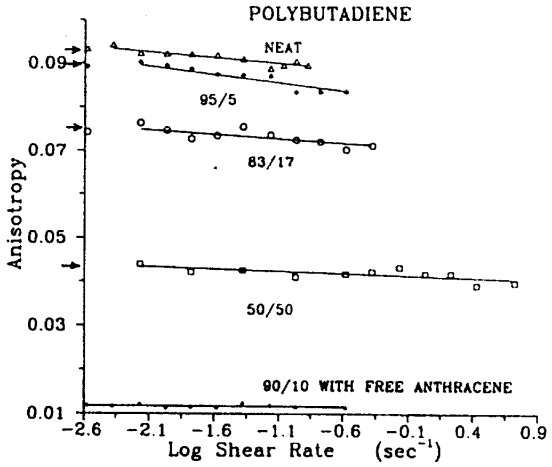

Figure 6. Anisotropy versus shear rate plotted for four PB specimens which were doped with 0.1% of the anthracene-tagged PB. The designations 95/5, 83/17, and 50/50 refer to PB which was plasticized with 5, 17, and 50% cetane, respectively. The 90/10 specimen was PB plasticized with 10% cetane and doped with free anthracene. The arrows on the abscissa indicate that values of zero-shear anisotropy.

specimens show non-Newtonian behavior. The effect on the polymer matrix by the plasticizer was most apparent in the behavior of the 50/50 specimen which, at low shear rates, displayed a portion of the transition to a Newtonian plateau.

Figures 6 and 7 show r vs shear rate and r vs shear stress, respectively, for the neat and plasticized specimens which have been doped with the tagged PB probe. The r values scale at different levels for each specimen in accordance with the value of A as expressed in eq 27. This scaling effect is more easily seen for the case of monoexponential decay, eq 29, where r_{cw} scales with the τ_r which becomes smaller with increasing plasticizer content. The decrease in anisotropy with shear rate and stress for the neat, 95/5, and 83/17 specimens is small but significant. The data for the neat specimen were affected by an experimental artifact, namely, poor contact between the specimen and the plates of the rheometer resulting in slippage. Because of this, we concentrated our attention on the behavior of the plasticized specimens whose tacky consistency produced good contact with the cone and plate surfaces. In Figure 7, r versus shear stress is shown for the 95/5, 83/17, and 50/50 specimens and for the control specimen, a 90/10 plasticized specimen doped with free anthracene. The standard deviation of these data is approximately twice

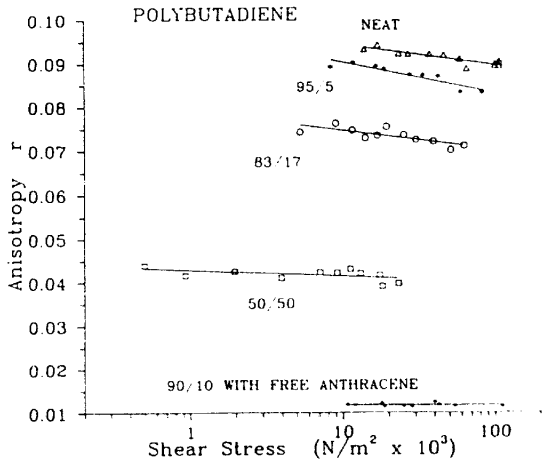

Figure 7. Anisotropy versus shear stress plotted for four PB specimens which were doped with 0.1% of the anthracene-tagged PB. The designations 95/5, 83/17, and 50/50 refer to PB which was plasticized with 5, 17, and 50% cetane, respectively. The 90/10 specimen was PB plasticized with 10% cetane and doped with free anthracene.

Table I
Summary of Zero-Shear Anisotropy Data

matrix polymer	M_w	% solute in cetane	r_0	τ_r, ns
PB	420 000	neat	0.0935	6.95
		95	0.0897	6.47
		83	0.0763	4.99
		50	0.0423	2.24
		20	0.0350	1.78
		0	0.0315	1.58
PB	24 000	neat	0.0860	6.03

the size of the data point. Within this range of uncertainty, the slopes of the 50/50 and free anthracene specimen curves are zero.

Also shown in Figure 6 are the zero-shear anisotropy values, indicated by the arrow and listed in Table I. It is assumed that these data are obtained under conditions of random orientation and that eq 28 applies. If we use $\tau_f = 9.4$ ns,[3] then τ_r can be calculated from eq 28. The values of τ_r range from 1.58 to 6.95 ns as the composition of the specimens change from dilute cetane solution to neat PB. Over this composition range, the macroscopic viscosity changed by over 10 orders of magnitude but the effect on τ_r was less than a factor of 5. Also shown in Table I are data for τ_r from two PB specimens differing in molecular weight by a factor of 20; only a small change in τ_r (15%) was observed, indicating that τ_r is independent of molecular weight. The lower value of τ_r in the 24 000 molecular weight specimen can be attributed to the plasticizing effect of the end groups.

Anisotropy measurements obtained using the cross-linked specimen are shown in Figure 8. In contrast to that observed for the specimens undergoing shear stress, these data display a positive slope in the r versus extension curve. The observation is in qualitative agreement with published data by Monnerie and co-workers, who examined anisotropy/extension effects using a similar fluorescent probe.[7,19]

Discussion

The rotational motion of the anthracene absorption dipole, which is directed along the polymer backbone, is the source of the relaxation time observations listed in Table I. The local mode character of the relaxation is exhibited in several ways. First, the relatively small difference between τ_r for a dilute cetane solution and neat

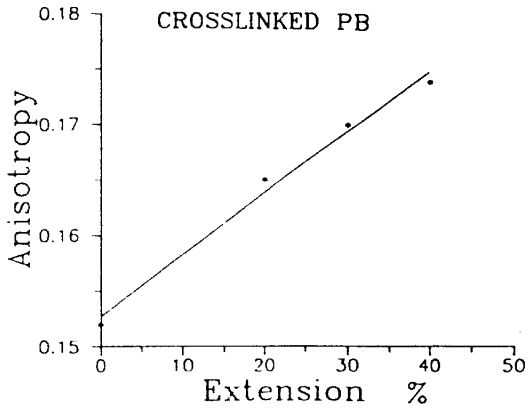

Figure 8. Anisotropy versus extension plotted for a cross-linked PB specimen containing 0.1% anthracene-tagged PB.

PB compared to the difference of more than 10 orders of magnitude change in the macroscopic viscosity of these two specimens indicates that τ_r is essentially independent of the macroscopic behavior and the establishment of the matrix polymeric entanglement network. Second, τ_r for the dilute-solution specimen is much smaller than $\tau_0 = 2M[\eta]\eta_0/2RT$, the zero-mode relaxation time for tumbling of the whole tagged PB molecule in dilute solution. Here, $[\eta]$ is the intrinsic viscosity and η_0 is the viscosity of the cetane; for 30 000 molecular weight PB in cetane, $\tau_0 = 700$ ns. Third, by measuring r as a function of temperature in the vicinity of room temperature, we calculated the activation energy for the relaxation of the neat specimen to be 3 kcal/mol, typical of the local-mode relaxation.[3] Finally, as we noted above, τ_r is independent of molecular weight. Considering that the entanglement molecular weight for PB is 2000–3000 (38–57 monomers), the local mode of relaxation being observed here has a correlated spatial length less than this distance.

Published data from time-resolved anisotropy decay experiments using similar tagged polymeric probe molecules show that, for both dilute-solution and neat specimens, the relaxation can be described by two relaxation times differing by a factor of approximately 10.[2-4,20-22] Extensive analysis of these data using model descriptions of the motion, particularly models of Hall and Helfand[23] and Bendler and Yaris,[24] verifies the local character of the relaxation which involves only a short section of the chain and is uncorrelated with the long-range modes of polymer chain motion. The Hall and Helfand model provides a molecular basis for the relaxation motion; the two relaxation times reflect correlated and isolated conformational transitions, where correlated transitions refer to local conformational changes that do not require translation or orientation of the chain end and isolated conformational transitions refer to translations of a short section of the chain. On the basis of the local character of the molecular motion, we make the assumption that the relaxation is uncorrelated with small orientations of the entanglement network which develop under shear loading and that τ_r and/or the value of A are independent of the applied shear stress. We conclude that the observed shear-induced changes in r are due to orientation of the fluorophore attached to the polymer chain and reflect chain segment orientation in its neighborhood. (We also assume that τ_f is independent of the shear stress; such an assumption is reasonable and has been made by Monnerie and co-workers for the case of molecular probes undergoing extensional stress, a stress environment more severe than that expressed here.[7,19,25])

The experiment with the control specimen illustrated that engagement of the probe molecule in the entanglement network is a necessary condition for observing a change in anisotropy over the range of shear stress employed here. Anisotropy was observed to be independent of the shear stress over the range of stress for which anisotropy of specimens having fully engaged host/probe entanglements decreased. We interpret these data to reflect the fact that free anthracene cannot orient with the matrix and that its relaxation time is unaffected by the application of shear stress.

Flow birefringence studies of cone and plate rheometry, carried out for a light beam perpendicular and parallel to the velocity gradient, show that orientation is imposed on a polymer specimen both by shear stress σ_{yz} and normal stress differences $(\sigma_{jj} - \sigma_{ii})$.[26,27] These stresses effect a distribution $f(\theta,\phi)$ of chromophore absorption dipoles with orientation both in and out of the plane of shear. In principle, anisotropy measurements yield three-dimensional information about $f(\theta,\phi)$. This is true for any placement of the excitation and emission polarizers. Equations 24, 25, and 27, however, hold only for the geometry used in this experiment, i.e., an excitation light beam parallel with the velocity gradient and an emission analyzer perpendicular to the excitation light beam.

Orientation of the entanglement network controls the development of $f(\theta,\phi)$ and the dependence of the orientation factors of eqs 24 and 25 on applied stress. The data of Figure 7 for the 5% plasticized specimen indicate that, as engaged entanglements produce molecular orientation with increasing shear rate and shear stress, the combined orientation terms decrease from $^2/_5$, the value at random orientation. We ask the question: does there exist a distribution function $f(\theta,\phi)$ which reflect orientation and causes anisotropy to decrease at small initial orientations? We consider the function

$$f(\theta,\phi) = 1 - \epsilon \cos^2\theta \cos^2\phi \qquad (34)$$

where $\theta = \theta_a$, $\phi = \phi_a$, and ϵ is a small number and a function of applied shear stress, σ_{13}. When $\epsilon = 0$, $f(\theta,\phi)$ describes random orientation, and for finite small ϵ, $f(\theta,\phi)$ describes an orientation slightly perturbed from the random distribution. Increasing values of ϵ correspond to increasing orientation. If we use $f(\theta,\phi)$ of eq 34 to calculate the orientation factors of eqs 24 and 25 as they are expressed in eq 27, then r_{cw} decreases with increasing ϵ, in accordance with our observations. Using $\epsilon(\sigma_{13})$ as the fitting parameter, a linear fit of eq 27 to the r vs shear stress data for specimen 95/5 yielded the relationship $\epsilon = 3.44 \times 10^{-7}\sigma_{13}$ (σ_{13} in N/m^2), where ϵ varied from 0 at $\sigma_{13} = 0$ to 0.024 at $\sigma_{13} = 6.86 \times 10^4$ N/m^2. Here, we used $A = 0.41$, a value obtained from zero-shear data. The fit of the data confirms the assumption that ϵ is a small number and that the distribution under steady-state stress is only slightly different than random. Although $f(\theta,\phi)$ is not a unique distribution function, it reflects a reasonable description of small shear-induced orientations and it demonstrates that the negative slope of the r versus shear stress data arises from the functional character of $f(\theta,\phi)$ and the resultant combination of orientation factors.

We interpret the results for the 50% plasticized specimen in terms of the entanglement molecular weight which increases from approximately 3100 for the 5% plasticized specimen to 6000 for the 50% specimen. For the 30 000 molecular weight probe, this means a decrease from approximately 10 entanglements per chain when incorporated in the 5% plasticized material to approximately five per chain in the 50% plasticized specimen. The anisotropy data for the two specimens when compared at equivalent applied shear stress show that the ability of the probe molecule to follow the orientation of the matrix is severely diminished in the 50% plasticized material. We see in the data of Figure 7 that the slope of anisotropy vs shear stress is near zero at 50% plasticization.

The observation that r decreased with applied shear stress is opposite to that which has been observed for extensional stress.[7,19] The major difference between uniaxial extension and shear flow is the combination of orientation factors which contribute to the observed anisotropy. For extension, uniaxial symmetry can be invoked, eliminating ϕ dependence as seen in eqs 31 and 32.[9,11,12] Our experimental observations indicate that $f(\theta,\phi)$ develops from the imposed stress in such a way that the resultant combination of orientation factors causes r to decrease with shear stress. The extension experiments were carried out for the purpose of verifying that the behavior of the tagged PB under extensional loading was in agreement with published results from similar experiments. We obtain qualitative confirmation of this agreement; i.e., anisotropy increases with extension. Analysis of the data involves the use of eqs 2, 31, and 32 in conjunction with an independent measurement of $\Psi(t)$. We need to separate the effects of orientation and changes in $\Psi(t)$ because it is inappropriate to assume that the relaxation time is constant for extension of a cross-linked material. The experimental challenge here is to measure relaxation time directly. This will be done in future work via time-resolved anisotropy decay observations.

Conclusions

We have demonstrated that a polymeric fluorescent molecule can be used to probe the shear-induced orientation of a polymer melt. This was done by synthesizing an anthracene-tagged polybutadiene probe molecule, doping it into a polybutadiene host matrix at a low concentration, and observing fluorescence anisotropy as a function of shear stress. By using a control specimen, free anthracene doped into high molecular weight PB, and by diluting the high molecular weight PB with plasticizer, we showed that engagement of the probe molecule in the host entanglement network is a necessary condition for observing shear-induced effects. We observed that fluorescence anisotropy of doped high molecular weight PB decreased with increasing shear stress. These observations were interpreted in terms of a derived relationship between anisotropy and the orientation factors of $f(\theta,\phi)$, the spatial distribution of absorption dipoles. An assumed $f(\theta,\phi)$, which was used to fit the anisotropy versus shear stress data, indicated that the shear-induced distribution was slightly perturbed from a random distribution. Shear-induced anisotropy effects were contrasted with extension effects which showed that anisotropy increases with increasing extension.

References and Notes

(1) Valeur, B.; Monnerie, L. *J. Polym. Sci., Polym. Phys. Ed.* **1976**, *14*, 11.
(2) Viovy, J. L.; Monnerie, L.; Melora, F. *Macromolecules* **1985**, *18*, 1130.
(3) Sasaki, T.; Yamamoto, M.; Nishijima, Y. *Macromolecules* **1988**, *21*, 610.
(4) Ricka, J.; Gysel, H.; Schneider, J.; Nyffenegger, R.; Binkert, T. *Macromolecules* **1987**, *20*, 1407.
(5) Chapoy, L. L.; Spaseska, D.; Rasmussen, K.; DuPre, D. B. *Macromolecules* **1979**, *12*, 680.
(6) Chapoy, L. L.; DuPre, D. B. *J. Chem. Phys.* **1979**, *70*, 2550.
(7) Jarry, J. P.; Monnerie, L. *J. Polym. Sci., Polym. Phys. Ed.* **1980**, *18*, 1879.

(8) Bower, D. I.; Korybut-Daszkiewicz, K. K. P.; Ward, I. M. *J. Appl. Polym. Sci.* **1983**, *28*, 1195.
(9) Jarry, J. P.; Monnerie, L. *J. Polym. Sci., Polym. Phys. Ed.* **1978**, *16*, 443.
(10) Chapoy, L. L.; DuPre, D. B. *J. Chem. Phys.* **1978**, *69*, 519. See also: Chapoy, L. L.; DuPre, D. B. in *Methods of Experimental Physics*; Fava, R. A., Ed.; Academic Press: New York, 1980; Vol. 16A.
(11) Zannoni, C. *Mol. Phys.* **1979**, *38*, 1813.
(12) Szabo, A. *J. Chem. Phys.* **1980**, *72*, 4620.
(13) Bur, A. J.; Lowry, R. E.; Roth, S. C.; Thomas, C. L.; Wang, F. W. *Macromolecules* **1991**, *24*, 3715.
(14) Brink, D. M.; Satchler, G. R. *Angular Momentum*; Oxford University Press: London, 1962.
(15) Wallach, D. *J. Chem. Phys.* **1967**, *47*, 5258.
(16) Perrin, F. *J. Phys.* **1926**, *1*, 390.
(17) Identification of a commercial product is made only to facilitate experimental reproducibility and to describe adequately experimental procedure. In no case does it imply endorsement by NIST or imply that it is necessarily the best product for the experiment.
(18) Colby, R. H.; Fetters, L. J.; Graessley, W. W. *Macromolecules* **1987**, *20*, 2226.
(19) Fajolle, R.; Tassin, J. F.; Sergot, P.; Pamburn, C.; Monnerie, L. *Polymer* **1983**, *24*, 379.
(20) Viovy, J. L.; Monnerie, L.; Brochon, J. C. *Macromolecules* **1983**, *16*, 1845.
(21) Viovy, J. L.; Frank, C. W.; Monnerie, L. *Macromolecules* **1985**, *18*, 2606.
(22) Hyde, P. D.; Waldow, D. A.; Ediger, M. D.; Kitano, T.; Ito, K. *Macromolecules* **1986**, *19*, 2533.
(23) Hall, C. K.; Helfand, E. *J. Chem. Phys.* **1982**, *77*, 3275.
(24) Bendler, J. T.; Yaris, R. *Macromolecules* **1978**, *11*, 650.
(25) Jarry, J. P.; Erman, B.; Monnerie, L. *Macromolecules* **1986**, *19*, 2750.
(26) Dexter, F. D.; Miller, J. C.; Phillippoff, W. *Trans. Soc. Rheol.* **1961**, *V*, 193.
(27) Osaki, K.; Bessho, N.; Kojimoto, T.; Kurata, M. *J. Rheol.* **1979**, *23*, 457.

Registry No. PB (homopolymer), 9003-17-2; $H_3C(CH_2)_{14}CH_3$, 544-76-3.